Numerical Simulation of ISFET Structures for BioSensing Devices with TCAD Tools

Daniele Passeri[1], Arianna Morozzi[1], Keida Kanxheri[1], Andrea Scorzoni[1]

[1]Dipartimento di Ingegneria Elettronica e dell'Informazione
Università degli Studi di Perugia
via G. Duranti 93, Perugia (Italy)
daniele.passeri@unipg.it

Abstract. Ion Sensitive Field Effect Transistors (ISFETs) are one of the primitive structures for the fabrication of biosensors (BioFETs). Aiming at the optimization of the design and fabrication processes of BioFETs, the correlation between technological parameters and device electrical response can be obtained by means of an electrical device-level simulation. In this work we present a numerical simulation approach to the study of ISFET structures for bio-sensing devices using Synopsys Sentaurus Technology Computer-Aided Design (TCAD) tools. In particular, we concentrate on the analysis of the field effect on the conduction channel of a general BioFET structure. This effect leads to the current modulation due to the fixed charges induced by immobilization of target biomolecules in an electrolyte environment.

Keywords: ISFET, numerical simulation, TCAD, biosensors.

1 Introduction

The integration of biologically active materials, such as molecules (enzymes, antibodies, antigens, proteins or nucleic acids) and/or biological systems (cells, plants, tissues, organs) with Ion Sensitive Field Effect Transistors (ISFETs) is one of the key elements for the fabrication of the class of biosensors referred to as BioFETs. The aim is to build an hybrid functional system, able to couple the unique (bio)receptor system capabilities with an electrical read-out and acquisition system. Silicon Field Effect Transistors (FETs) are nowadays the primitive element of the new generation of biosensors, since BioFETs can be built from the basic ISFET structure by modifying the gate of the transistor or by coupling the gate oxide with biological sensing elements (receptors).

Aiming at the optimization of the design and fabrication processes of BioFETs, the correlation between technological parameters and device electrical response should more directly be obtained by means of an electrical device-level simulation. To this purpose, different approaches have been proposed in literature both at device and circuit level [1, 2, 3]. In particular, in the approach proposed in [3] the incorporation of a physical model of the electrolyte-insulator-semiconductor (EIS) structure into a

numerical device simulator has been carried out. The EIS system equations are coupled with the charge-transport equations and solved self-consistently on the discretized domain, thus resulting in a “custom” simulation tool.

In this work, we rely on the state-of-the-art commercial Synopsys Sentaurus TCAD packages. Sentaurus is a suite of TCAD tools which simulates the fabrication, operation and reliability of semiconductor devices [4]. The Sentaurus simulators use physical models to represent the device fabrication steps and operation, thereby fostering the exploration and optimization of new semiconductor devices. The adoption of TCAD tools reduces technology development time and cost at the same time providing insight into advanced physical phenomena through self-consistent multidimensional modelling capabilities, improving device design, yield, and reliability. However, the direct device level simulation of an electrolyte solution in Sentaurus TCAD is not straightforward: actually, the suite of standard materials does not include any electrolyte.

The properties of a custom-defined material were therefore modified in order to reproduce the electrolyte behavior. In particular, the parameters of an intrinsic semiconductor material have been set in order to reproduce an electrolyte solution: the permittivity and the refractive index were set in order to reproduce the behavior of water. The bandgap energy dependence on the temperature is modelled as

$$E_g(T) = E_g(0) - \frac{\alpha T^2}{T+\beta} \quad (1)$$

were α and β are material dependent parameters and $E_g(0)$ is the bandgap energy at $T = 0\text{K}$. We set the $E_g(0) = 1.5$ eV thus satisfying the requirement $\left(E_g/2 - q\varphi\right) \gg kT$, i.e. greater than a few thermal energies (q is the elementary charge and φ is the electrical potential of the material). With this approximation the Poisson–Boltzmann (PB) equation, describing the charge distribution in the electric double layer, can be viewed as the semiconductor equation applied to an intrinsic material [5]. By replacing the electrolyte solution with an intrinsic semiconductor, the electrostatic solution of the electrolyte region can therefore be calculated by solving the semiconductor equation within this region.

The Shockley–Read–Hall (SRH) statistics has been adopted for the generation/recombination processes modelling, by setting the maximum recombination time according to literature findings [6]. In order to account for the surface effects on the carrier mobility, the simplified Lombardi model was used [4]. Actually, in the channel region of a FET, the high transverse electric field forces carriers to interact strongly with the semiconductor–insulator interface. Carriers are subjected to scattering by acoustic surface phonons and surface roughness. This model can describe the mobility degradation caused by these effects; the maximum mobility values have been set to $\mu_n^{max} = 6.88 \cdot 10^{-4}\,\text{cm}^2/\text{V}\cdot\text{s}$ and to $\mu_p^{max} = 4.98 \cdot 10^{-4}\,\text{cm}^2/\text{V}\cdot\text{s}$ respectively, to reproduce the behavior of Na^- and Cl^+ ions in a $NaCl$ solution [6]. It should be noticed that the carrier mobility is much lower with respect to standard free carrier mobility of an intrinsic semiconductor, thus consistently miming the behavior of ions in a real ionic solution.

Eventually, the most significant parameters that correlate the physical properties of an electrolyte solution to the electrical parameters of an intrinsic semiconductor are the semiconductor state densities within the conduction and the valence bands, N_C and N_V, respectively. Within this framework, the electrons and holes represent the mobile ions in the solution. The density of states N_C and N_V were therefore specified according to the molar concentration of the ionic solution, according to the following procedure. If we consider the H_2O dissociation $H_2O + H_2O \rightarrow H_3O^+ + OH^-$ at the chemical equilibrium, the concentration of $[OH^-]$ and $[H_3O^+]$ are correlated by the ionic product for water

$$K_W = [H_3O^+][OH^-] \qquad (2)$$

This value is strongly dependent on the temperature; however, at T=25 °C it reads $K_W = 10^{-14}$ [7]. The analogy with the electrons and holes concentrations in a semiconductor can be accomplished by accounting for the *mass action law,* stating that under thermal equilibrium the product of the free electron concentration n and the free hole concentration p is equal to a constant equal to the square of intrinsic carrier concentration. If the number of carriers is much less than the number of band states, the carrier concentrations can be approximated by using the Boltzmann statistics, giving

$$n \cong N_C e^{-\frac{E_C - E_f}{kT}} \qquad (3)$$

and

$$p \cong N_V e^{-\frac{E_f - E_V}{kT}} \qquad (4)$$

where E_C is the lower energy limit of the conduction band, E_V is the upper energy limit of the valence band, E_f is the Fermi level and k is the Boltzmann constant. By combining (3) and (4) if $n = p$

$$np = N_C N_V e^{-\frac{E_G}{kT}} = n_i^2 \qquad (5)$$

The effective density of states for electrons in the conduction band and for holes in the valence band are calculated from $N_C = 2\left[\frac{2\pi m_e^* kT}{h^2}\right]^{3/2}$ and $N_V = 2\left[\frac{2\pi m_h^* kT}{h^2}\right]^{3/2}$ where m_e^* and m_h^* are the effective mass of electrons and holes for density of states calculations, and h is the Planck constant.

For the calculation of the electrolyte "equivalent" semiconductor N_C and N_V values, we can consider the Avogadro constant $N_A = 6.022 \cdot 10^{23}\text{mol}^{-1}$ to convert $1\text{mol/L} \rightarrow 6.022 \cdot 10^{23}[\ ]/\text{L} \rightarrow 6.022 \cdot 10^{20}[\ ]/\text{cm}^3$ and assuming $[H_3O^+] \equiv p, [OH^-] \equiv n$. Therefore, for instance, for a solution with $pH = 7$ the concentration of the ion $[H_3O^+] = 10^{-7}$ mol/L corresponds to the hole concentration $p = 10^{-7} \times 6.022 \cdot 10^{20}\ [ions]/\text{cm}^3 = 6.022 \cdot 10^{13}\ [ions]/\text{cm}^3$. By substituting this value in the expression (4), the "equivalent" density of states in the valence band can be calcu-

lated, by considering, as previously introduced, the energy gap $E_g = 1.5$ eV and obtaining

$$N_V = 2.4 \times 10^{26}\text{cm}^{-3}. \quad (6)$$

A similar procedure can be used to determine the density of states in the conduction band. For a $pH = 7$ the concentration of both ion species are the same, i.e. $[H_3O^+] = [OH^-]$ therefore we calculate $n = 10^{-7} \times 6.022 \cdot 10^{20}\,[ions]/\text{cm}^3 = 6.022 \cdot 10^{13}\,[ions]/\text{cm}^3$ corresponding to

$$N_C = 2.4 \times 10^{26}\text{cm}^{-3}. \quad (7)$$

The relations (6) and (7) hold for a $pH = 7$ solution. However, this is not a limiting case. By considering the ionic product of water, the ionic species concentrations can be translated to carrier concentrations, depending on the concentration of the solution. In other words, for any given pH value of an equilibrium state solution at a constant temperature T, it is possible to determine the concentration of n and p of the equivalent intrinsic semiconductor, and therefore the values of N_C and N_V.

In order to check the suitability of the modelling procedure, an ISFET device has been simulated. The 2D cross-section of the simulated structure is reported in Fig. 1, along with its discretization mesh. The static characteristic of the device, namely the $I_D - V_{DS}$ curves for different biasing voltages of the reference electrode are reported in Fig. 2. The qualitative behaviour of the devices is very similar to the classical MOSFET $I_D - V_{DS}$ curves, as expected.

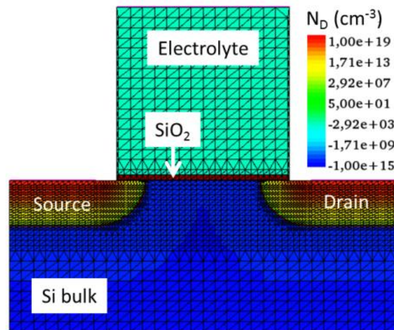

Fig. 1. Cross-section of the simulated ISFET device

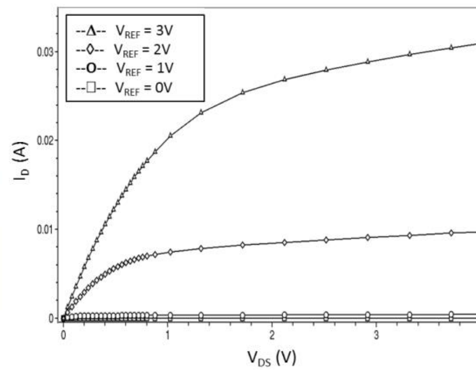

Fig. 2. Output characteristics of the ISFET device

By varying the solution pH, e.g. the concentration of ionic species, the sensitivity of the ISFET device as pH sensor can be evaluated (Fig. 3). By considering a reference value of $V_{DS} = 2$ V, the family of curves of the drain current as a function of the reference electrode voltage can be calculated, by varying the densities of states of the electrolyte material according to the solution pH. A sensitivity of 60 mV$/pH$ in terms of threshold voltage shift has been found, in agreement with literature data [3, 6].

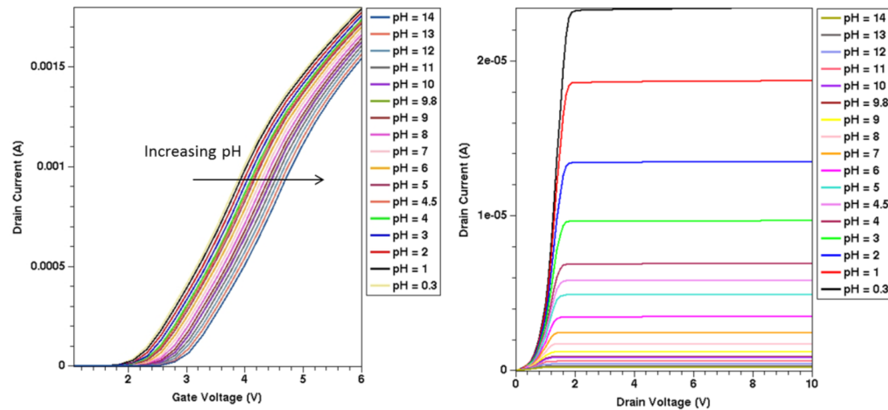

Fig. 3. Drain current as a function of the reference electrode voltage (left) and as a function of the drain voltage (right) at different pH solution concentrations

2 Device Simulation of a Sample BioFET Device

Once assessed the suitability of the methodology, a physically sound modelling scheme of BioFET sensors has been set-up. The label-free electrical biosensors rely on the field effect induced by charges of target biomolecules in an electrolyte environment. In real devices, receptor probes are immobilized on the surface of an electrolyte-insulator-semiconductor system so that the target molecules are bound to the probes by the bio-affinity phenomenon. The localized, fixed charges induce the field effect on the underlying conduction channel that leads to the current modulation. The channel modulation effect induced by irregular charge distribution can scarcely be estimated through analytical methods. Moreover, significant effect have been observed at very low target concentration when only a small portion of the receptor probes is bound to the target molecules. On the other hand, the detailed analysis of the effect of the actual charge distributions could conveniently be obtained through an accurate numerical simulation method [5]. The proposed methodology guarantees the self-consistent modelling of very different types of material regions, such as semiconductor, electrolyte solution and organic molecule regions. In particular, a realistic picture of the charge distribution can be obtained as a cluster of charges on the electrolyte region due to target molecules which are bound randomly to a receptor site. When a binding reaction occurs at a certain position on the surface, a given charge density is localized in that specific position.

In this work, we propose this methodology to the study of electrophysiological neuronal activity. It has been already pointed out in the past that ISFET devices can measure the extracellular voltage of a single neuron attached with its cell membrane to the device insulator in an open gate configuration [7, 8, 9]. The change of the extracellular voltage induced by the neuron gives rise to an electric field across the insulator that modulates the drain-to-source current of the ISFET [10].

A sample simulated structure is therefore shown in Fig. 4. The whole system is based on a standard ISFET device, featuring a p-type low doped Si substrate, a thin SiO_2 interface and an electrolyte solution with a top reference electrode. The effect of spatially localized charges due to immobilization of target molecules is reproduced by means of a number of small blocks of dielectric material whose dimensions are compatible with the dimension of the target cells (we assume that the shape of the cell does not affect the charge distribution). The dimensions of the blocks and their distance from the dielectric surface can be chosen as design parameters, in order to account for different kinds of biosensors (e.g. target specificity and/or electrolyte characteristics which define the receptor size and position). When the affinity reaction occurs at the receptor site (i.e., receptor and target molecule bind creation), a given charge distribution is created to each single block. The charge state of each block can be therefore neutral ($Q = 0$) or charged ($Q = Q_T$). In this case, a value of $Q_T = 4.8 \cdot 10^{-16} C$ has been used.

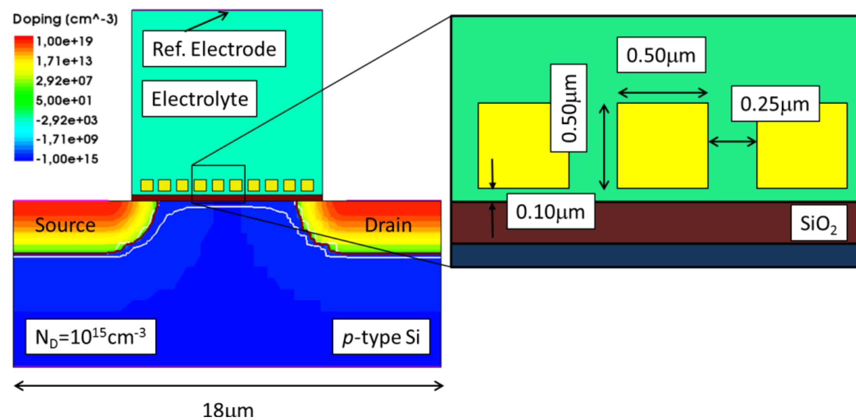

Fig. 4. Sketch of the simulated structure: charge localization at the SiO_2 surface is modelled with localized dielectric block with or without charge

The electrostatic behaviour (transfer characteristics) of the structure has been simulated when the captured target number increases from 1 to 10. In a random distributed charge modelling, however, the static characteristics cannot be represented by a single curve. Actually, the transistor channel can have different conductance values depending on the bound target positions despite the fact that the number of bound targets (Fig. 5) is the same. Since the conductance does not have a linear relationship with the target charge, the overall conductance modulation cannot be obtained through a linear combination of the modulation effects induced by each target. Therefore, one should simulate every case of the receptor–target binding combination to obtain a complete set of conductance results. This is of course an overwhelming computational effort; we therefore simulated a still huge number of several randomly selected sample cases.

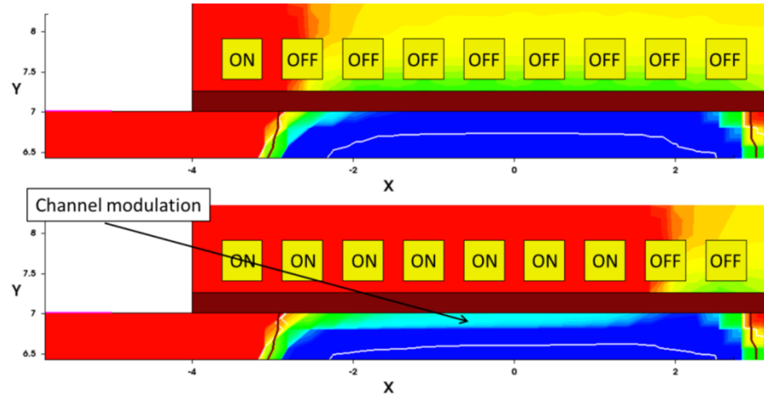

Fig. 5. Channel modulation as a function of the number of the occupied receptors

In Fig. 6 is shown the I_D current as a function of the V_{DS} voltage for different positions of a single charged block. The reference electrode voltage was set to ground, e.g. $V_{REF} = 0$ V. Starting from the lower curve (when no localized charge at all is experienced, i.e. when no reaction has occurred), the current tends to increase with the position of the charged block moving from the source channel region (C1 *on*) toward the middle between source and drain (C5 *on* or C6 *on*), and eventually decreasing when the charge approaches the drain region (C10 *on*).

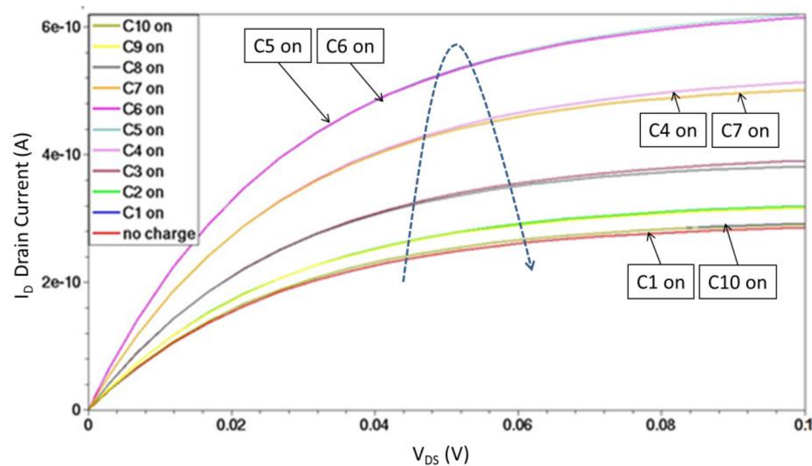

Fig. 6. Drain current as a function of the reference voltage, depending on the position of a single charged receptor

As mentioned before, the distribution of the charge has a strong effect on the channel modulation. For instance, if we consider three receptors *on*, localized near the source region or randomly distributed along the channel region, significantly different currents have been calculated, namely a marked increase of the current is experienced

(more than one order of magnitude) when the turned on charges are more distributed along the bind sites (Figs. 7 and 8).

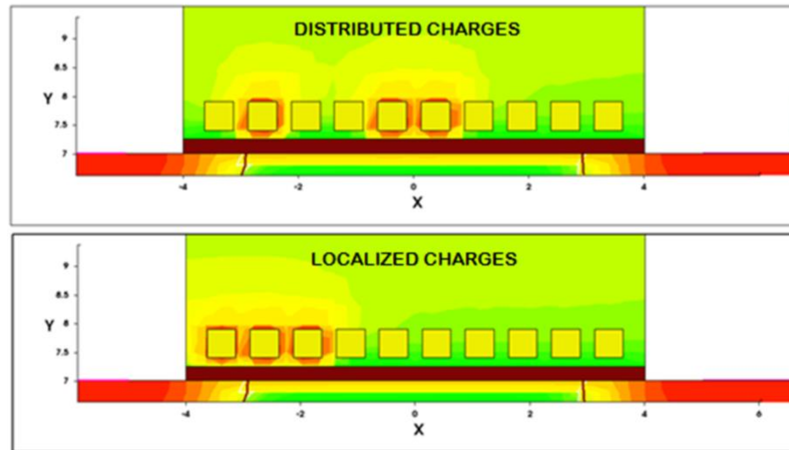

Fig. 7. Localized vs. distributed charged receptors

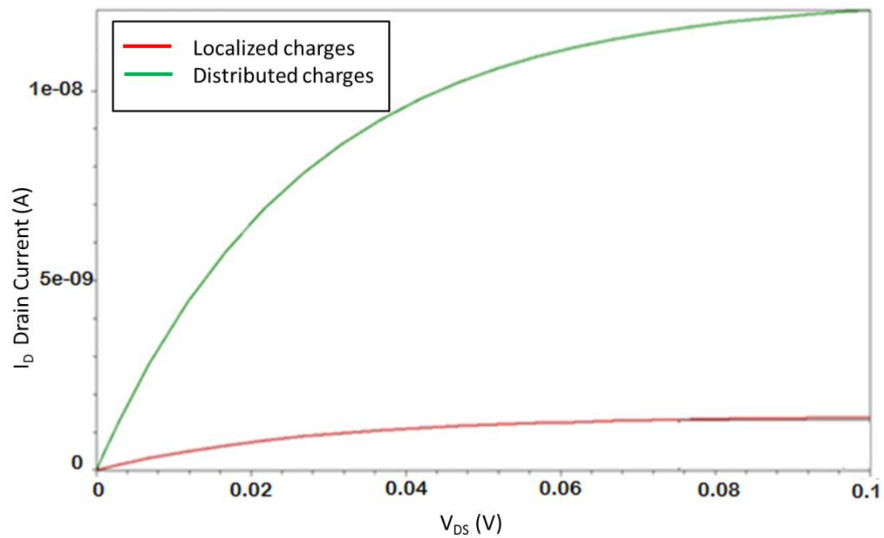

Fig. 8. Drain current as a function of the reference electrode voltage with three active receptors: localized vs. distributed charged receptor effect on the I_D current

An overall effort aiming at summarizing the current modulation effects of an increasing number of localized charges is shown in Fig. 9. The relationship between current modulation and target number is not linear at all. Actually, the position of the

targets has a strong effect: for instance, the localization of few targets turned on can result in a greater current modulation with respect to even a bigger number of grouped active targets. In general, charges localized near the source and drain region (C1 and C10 in the example at hand) are less effective, since the modulation of the channel is mostly affected by the influence of the lateral diffusion of source and drain region implants. Moreover, charges localized near the source (C2, C3) are more efficient in current modulation with respect to charges localized near the drain (C8, C9).

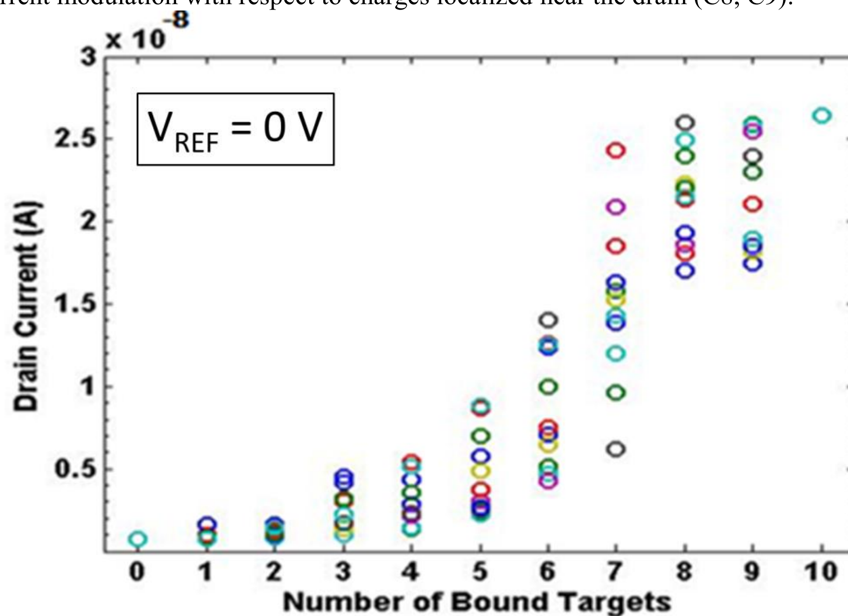

Fig. 9. Drain current as a function of the number of charged receptors: coloured circles in each column (e.g. for the same number of charged receptors) correspond to different random position combinations ($V_{DS} = 100mV$, $V_{REF} = 0V$)

A further significant effect on the electrical current values is due to the reference electrode voltage. If we increase the reference voltage, a marked increase of the current (around four orders of magnitude) has been calculated. This is due to the different conducting region of the equivalent FET transistor. Even if is not straightforward to determine its threshold voltage, when the $V_{REF} = 0V$ we are in sub-threshold region, namely in a very low current regime. On the other hand, when the $V_{REF} = 1$ V the transistor goes on, and a much greater current flows between source and drain even when a small V_{DS} voltage is applied. In both cases the conductive channel modulation effect is visible; a smaller modulation ratio (namely, the ratio I_D^{max}/I_D^{min} between the maximum current I_D^{max} when all receptors are on with respect to the minimum current I_D^{min} when no charge is applied) has been obtained when $V_{REF} = 1$ V (Fig. 10), but the bigger values of the current are a definite advantage, for instance allowing for a much simplified real experimental measurement setup. The same behaviour is further enhanced if a greater V_{REF} is used, e.g. $V_{REF} = 2$ V.

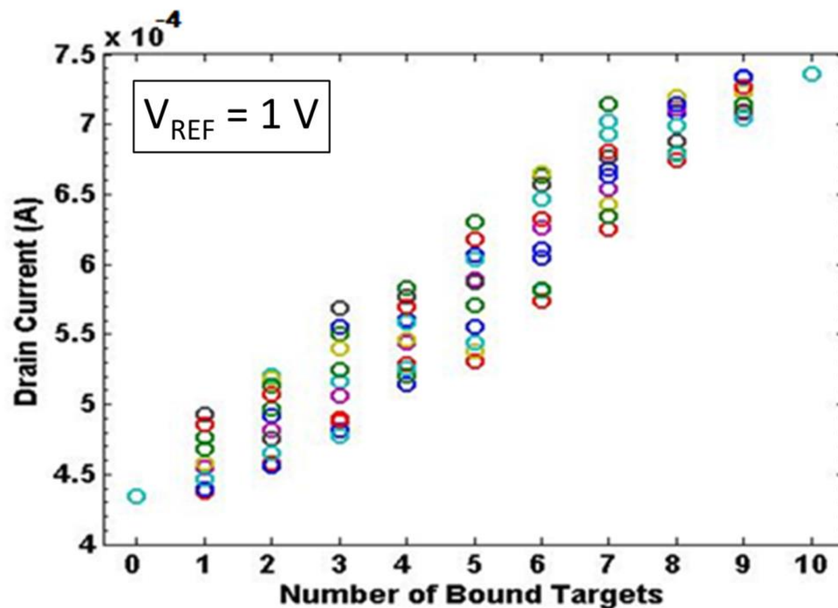

Fig. 10. Drain current as a function of the number of charged receptors: coloured circles in each column (e.g. for the same number of charged receptors) correspond to different random position combinations ($V_{DS} = 100$ mV, $V_{REF} = 1$ V)

Conclusions

In this work we presented a numerical simulation approach to the study of Ion-Sensitive Field Effect Transistor (ISFET) structures for biosensing devices (BioFETS) using the Synopsys Sentaurus Technology Computer-Aided Design (TCAD) tools. In particular, we concentrate on the analysis of the field effect on the conduction channel of a general BioFET structure that leads to the current modulation due to the fixed charges induced by immobilization of target biomolecules in an electrolyte environment. The channel modulation effect induced by irregular, locally distributed charges can be deeply investigated by means of device-level numerical simulation, as well as the effects of different electrolyte concentrations (pH) on the device sensitivity.

In this way a powerful framework for the design and optimization of biosensor can be devised, thus reducing technology development time and cost. The main finding of the analysis of a general reference BioFET shows that there is no linear relationship between the number of charges and the current modulation, but there is a strong position dependent effect: targets localized near the source region are most effective with respect to targets localized near the drain region, and in general even randomly distributed targets are more efficient with respect to locally grouped targets on the current modulation. The effect of the V_{DS} drain source voltage on the sensitivity of the device, as well as the effect of the different polarization of the electrolyte reference voltage (V_{REF}) can be studied in detail. In particular, for the device at hand, a small

positive biasing of the electrolyte solution, providing that the transistor goes on, will result in a greater enhancement of the current levels, still retaining a good sensitivity but greatly simplifying the operations of a real device.

References

1. M. Grattarola, G. Massobrio, and S. Martinoia, "Modeling H+-sensitive FET's with SPICE," IEEE Trans. Electron Devices, vol. ED-34, pp. 813–819, 1987.
2. W. Treichei, M. Ullrich, H. Voigt, M. Appei, R. Ferretti, "Numerical modeling and characterization of Electrolyte/Insulator/Semiconductor sensor systems," Journal of Analytical Chemistry, June II, Volume 349, Issue 5, pp 385-390, 1994.
3. L. Colalongo, G. Verzellesi, D. Passeri, B. Margesin, M. Rudan, P. Ciampolini, "Numerical analysis of ISFET and LAPS devices," Sensors and Actuators B, vol. B44, pp. 402-408, June 1997.
4. http://www.synopsys.com/Tools/TCAD/CapsuleModule/sentaurus_ds.pdf
5. In-Young Chung, Hyeri Jang, Jieun Lee, Hyunggeun Moon, Sung Min Seo, Dae Hwan Kim, "Simulation study on discrete charge effects of SiNW biosensors according to bound target position using a 3D TCAD simulator," Nanotechnology 23 (2012) 065202.
6. David Welch, Sahil Shah, Sule Ozev, and Jennifer Blain Christen, "Experimental and Simulated Cycling of ISFET Electric Fields for Drift Reset," IEEE Electron Device Letters, vol. 34, no. 3, March 2013.
7. Fromherz P., Offenhausser A., Vetter T., Weis J. , "Neuron-silicon junction: a Retzius cell of the leech on an insulated-gate field-effect transistor," J. A. Science 1991, 252, 1290–1293.
8. Vassanelli, S.; Fromherz, P. "Transistor-Records of Excitable Neurons from Rat Brain", Appl. Phys. A: Mater. Sci. Process. 1998, 66, 459–464.
9. Fromherz, P. "Neuroelectronic Interfacing: Semiconductor Chips with Ion Channels, Nerve Cells, And Brain", Nanoelectronics and Information Technology; Waser, R., Ed.; Wiley-VCH: Berlin, Germany, 2003; pp 781-810
10. Giuseppe Massobrio, Paolo Massobrio, and Sergio Martinoia, "Modeling the Neuron-Carbon Nanotube-ISFET Junction to Investigate the Electrophysiological Neuronal Activity," NANO LETTERS, 2008, Vol. 8, No. 12, 4433-4440.